Detection of dopamine using glassy carbon electrodes modified with AgNPs synthetized with *Monteverdia ilicifolia extract*

Francielle Schremeta Humacayo[1] ✉, Joel Toribio Espinoza[2] ✉, Josiane de Fátima Padilha de Paula[2] ✉, Luma Clarindo Lopes[1] ✉, Christiana Andrade Pessoa[1] ✉, Cássia Gonçalves Magalhães[1+]

1. State University of Ponta Grossa ROR, Department of Chemistry, Ponta Grossa, Brazil.
2. State University of Ponta Grossa ROR, Department of Science, Ponta Grossa, Brazil.

+Corresponding author: Cássia Gonçalves Magalhães, Phone: +55 42 3220-3062, Email address: cgmagalhaes@uepg.br

ARTICLE INFO

ABSTRACT: This work reports a new application for a well-known medicinal plant used in Brazil. The green synthesis of silver nanoparticles (AgNPs) using the aqueous extract of *Monteverdia ilicifolia* (MI) leaves as stabilizing and reducing agent is described. The AgNPs-MI obtained were characterized by UV-VIS, FTIR, and Raman spectroscopies, DLS, zeta potential and FEG-SEM, which demonstrated that *M. ilicifolia* was effective at capping the AgNPs, yielding stable suspensions. These nanoparticles were deposited on glassy carbon electrodes, and they were efficiently applied as electrochemical sensors for the determination of dopamine (DA) using square wave voltammetry (SWV). The AgNPs-MI improved the electrochemical properties of the electrodes and enhanced their electroanalytical performance. The developed sensing device presented detection and quantification limits equal to 0.52 and 1.74 μmol L^{-1}, respectively, towards DA determination. The proposed electrochemical sensor quantified this neurotransmitter successfully, confirming its potential as a new promising analytical detection tool for DA quality control.
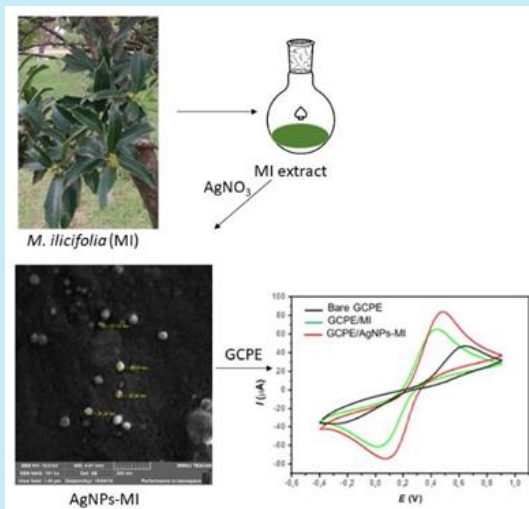
1. Introduction

The green synthesis of metal nanoparticles shows many advantages when it is compared to conventional methods, since natural compounds make these syntheses environmentally friendly, as well as cheaper processes (Huq *et al.*, 2022). Among the materials used in the biosynthesis of metal nanoparticles, the use of plants as reducing agents is widely explored, because it shows lower risks and provides a fast and stable product (Ahmad *et al.*, 2016a; Jadoun *et al.*, 2021). Considering the huge Brazilian biodiversity, it is possible to justify the interest of using the natural resource for the biosynthesis of metal nanoparticles, where species belonging to Celastraceae family constitute a good source for this technological application. For example, the extract of the root of *Monteverdia salicifolia* (syn. *Maytenus salicifolia)* was used as a stabilizing and reducing agent in the production of silver nanoparticles (AgNPs), with size in the range of 48–80 nm (Grzygorczyk *et al.*, 2021). The extract of *M. royleanus* leaves was useful in the synthesis of gold nanoparticles (AuNPs) with particles size of approximately 30 nm, which exhibited relevant antileishmanial activity (Ahmad *et al.*, 2016a). Moreover, the extract of the stems of this species lead to the synthesis of AgNPs associated to amphotericin B, with an approximate particle size of 15 nm. They exhibited higher antifungal activity than the nanomaterial that was not conjugated (Ahmad *et al.*, 2016b). According to the evidence, the research that aim to study the capacity of plant extracts in the synthesis of nanoparticles as well as the evaluation of these biological properties are very relevant.

The most known species from this genus is *Monteverdia ilicifolia*, popularly known in Brazil as *espinheira santa* and *espinho-de-deus*. It is endemic to southern Brazil, Argentina, Paraguay, and Uruguay. This species is largely used in the traditional medicine in the treatment of gastritis, ulcers, and other gastric disorders (Périco *et al.*, 2018; Zhang *et al.*, 2020). The use of this extract exhibited advantages when compared to the commercial drugs that acts inhibiting the proton pump, such as omeprazole, that leads to side effects (Tabach *et al.*, 2017).

The AgNPs also have attractive characteristics such as chemical stability, high surface area and relevant electrical and optical properties, being very versatile materials for different applications (Jadoun *et al.*, 2021). They can be applied specially in the modification of electrodes, to improve electroanalytical techniques, where they can allow new electrochemical properties to them, increasing their selectivity, sensibility and stability. In consequence, they become a useful tool for determination of specific compounds in biological samples and for the control of quality of drugs (Lima Filho *et al.*, 2019). In this context, many investigations highlighting the potential of plants improving the electrochemical properties of the electrodes have been reported. Screen-printed electrodes modified with Ag-NPs, which were biosynthesized using an extract aqueous of grape stalk waste, were tested for the simultaneous stripping voltammetric determination of Pb(II) and Cd(II). The results indicated good reproducibility, sensitivity and limits of detection around 2.7 µg L^{-1} for both metal ions (Bastos-Arrieta *et al.*, 2018). The extract of *Araucaria angustifolia* was effective as a reducing and stabilizing agent in the synthesis of AgNPs. These nanomaterials were applied to a glassy carbon electrode used for the determination of paracetamol in drugs (Zamarchi and Vieira, 2021). Besides, carbon paste electrode modified with banana tissue was effective for determination of catechol in green tea (Broli *et al.*, 2019). This evidence emphasizing the importance of the development of studies involving plants in order to extend their technological applications.

Dopamine (DA) is a neurotransmitter of the central and peripheral nervous system, responsible for physiological activities, such as behavior, memory, and movement. Abnormal levels of this catecholamine can lead to many neurological diseases, such as schizophrenia, Parkinson's disease and hyperactivity (Blum *et al.*, 2021). Thus, the development of very selective and sensitive techniques for monitoring the level of DA in the organism are very important. This neurotransmitter has a known voltammetric behavior which enables its determination by electrochemical methods (Selvolini *et al.*, 2019; Yu *et al.*, 2018). As an example, the detection of DA was made with a screen-printed carbon electrode modified by AuNPs derived from *Rhanterium suaveolens* flowers extract (Chelly *et al.*, 2021). A biosensor modified with AgNPs obtained from aqueous leaf extract of *Ziziphus mauritiana* was successfully applied for DA detection in real urine samples (Memon *et al.*, 2021).

At the best of our knowledge, the biosynthesis of AgNPs using the extract of *M. ilicifolia* leaves is not reported. Therefore, considering the significant therapeutic value of *M. ilicifolia* (RENISUS, 2009; Tabach *et al.*, 2017) the aim of this study was performing the green synthesis of AgNPs using the aqueous extract of its leaves and their application in the modification of glassy carbon electrodes, applied in the electroanalytical determination of DA.

2. Experimental

2.1 Plant extract

M. ilicifolia leaves were collected from a specimen located at campus of the Universidade Estadual de Ponta Grossa (UEPG, 25°5'23"S 50°6'23"W), in Ponta Grossa, Paraná, Brazil. A voucher specimen was deposited at UEPG Herbarium, under number HUPG 21178. This species was insert on SISGEN platform under register A8E6438.

The leaves (20.17 g) were dried, ground and mixed with 300 mL of distilled water. The mixture was submitted to heat to boiling. After this, the sample was filtered, getting to the aqueous extract, which was stored at 4 °C.

2.2 Synthesis and characterization of silver nanoparticles

The green synthesis of the AgNPs was performed with the addition of 1.0 mL of the aqueous extract collected of a stock solution (extract diluted in distilled water in the proportion of 1:10), to 19.0 mL of $AgNO_3$ 1.0×10^{-3} mol L^{-1}. This mixture was heated at 60 °C and stirred for 10 min. The AgNPs with *M. ilicifolia* (AgNPs-MI) synthetized were kept in light-protected vials.

The nanocomposites were characterized by ultraviolet-visible spectrophotometry (UV-VIS) (in a Cary 50 Varian spectrophotometer) by scanning the wavelengths in the range of 200–800 nm. FTIR spectra were recorded in attenuated total reflectance (ATR) mode in the scanning range of 4000–400 cm^{-1} (scan rate of 10 cm^{-1}) for AgNPs-MI and *M. ilicifolia* (10 mg mL^{-1} solution) KBr tables after lyophilization of the extract, at room temperature. Raman spectral analysis were obtained in a spectrometer Xplora Plus (HORIBA scientific) in a range of 100 to 2,000 cm^{-1}. A laser of 532 nm was chosen for the measurements.

Field emission gun-scanning electron microscopy (FEG-SEM) was done in a Myra 3 LMH Tescan microscope (15 mV: 356 mA). The particle diameter was obtained by dynamic light scattering (DLS) measurements on a Malvern NanoZ590 equipment.

2.3 Preparation of glassy carbon paste electrodes

The unmodified glassy carbon paste electrode (GCPE) was prepared by mixing 50.0 mg of glassy carbon powder with 10.0 µL of mineral oil until homogenization. After this, a portion of this mixture was inserted into the cavity of a Teflon tube. For the construction of the modified electrodes with -MI, different amounts of this nanocomposite (10.0, 25.0, 50.0, 75.0 and 100 µL) was mixed with 50.0 mg of glassy carbon powder. After homogenization, at this mixture 10.0 µL of mineral oil was added. Similarly, to the bare GCPE, the modified glassy carbon paste was packed into Teflon tubes. A carbon paste electrode modified with the plant extract was also prepared (GCPE/MI), using 50.0 µL of the aqueous extract of *M. ilicifolia* leaves, diluted with distilled water (1:10) with 50.0 mg of glassy carbon powder. In this case, the mixture was homogenized and dried under air flow, followed by the addition of 10.0 µL of mineral oil. After a new homogenization step, this modified carbon pastes were separately inserted into Teflon tubes, similarly to the others. The electrode surfaces were renewed by smoothing the resulting electrodes on a soft paper and then on a glass plate.

2.4 Electrochemical characterization

Electrochemical measurements were carried out at room temperature, using a conventional three-electrode cell system. The carbon paste electrodes (modified or unmodified), Ag/AgCl/KClsat electrode and a platinum spiral wire were used as working electrodes, reference and auxiliary, respectively. In order to characterize the modified electrodes, cyclic voltammetry (CV) and electrochemical impedance spectroscopy (EIS) experiments were performed in an Autolab PGSTAT 100 potentiostat/galvanostat, by employing 0.15 mol L^{-1} PBS solution containing 10.0 mmol L^{-1} $K_4Fe(CN)_6$/$K_3Fe(CN)_6$ as supporting electrolyte.

For DA determination with the GCPE/MI and GCPE/AgNPs-MI, CV and square wave voltammetry (SWV) measurements were conducted in a PalmSens potentiostat (Palm Instruments BV) in 0.04 mol L^{-1} BR buffer, in the pH range of 2.0 to 7.0; DA = 1.0 mmol L^{-1}. Analytical parameters such as sensitivity, repeatability, reproducibility, limit of detection (LOD), limit of quantification (LOQ), and accuracy were determined for the modified electrodes following the Brazilian Health Surveillance Agency (ANVISA (2003) and International Conference on Harmonization (ICH, 2005) guidelines. In appropriate conditions, the CPE/AgNPs-MI was studied in different scan rates (10–100 mV s^{-1}) to determine the type of mass transport that guide the oxidation of DA on the modified electrode.

3. Results and discussion

3.1 Synthesis and characterization of the AgNPs-MI

The biosynthesis of AgNPs using the aqueous extract of *M. ilicifolia* leaves was indicated by the color changing of the solution, from colorless to orange, which is a characteristic color of AgNPs in suspension. This show that the extract was able to reduce the cations Ag$^+$ in Ag^0 nanoparticles. It is important to emphasize that the advantage of using this extract in the nanoparticle synthesis is that it provides their both reduction and stabilization, and it is also an environmentally friendly and cheap reagent. Moreover, the AgNPs obtained were very stable, maintaining their size for about three months.

The color changing is due to the surface plasmon effect (Grzygorczyk *et al.*, 2021), exhibited for the AgMPs-MI. It is worth highlighting that the reaction time was very short, only 10 min, without the need to change the pH of the solution. The extract can act as both reducing agent and stabilizer simultaneously.

Studies about the phytochemical profile of *M. ilicifolia* show a great variety of secondary metabolites, such as pentacyclic triterpenes (friedelinol, friedelin, lupeol), phenolic acids and the flavonoids kaempferol, quercetin, epigallocatechin, among others (Périco *et al.*, 2018; Zhang *et al.*, 2020). Phenolic compounds, such as gallic acid and tannic acid, were useful as stabilizing and reducing agents in the synthesis of bimetallic Au@AgNPs (Orlowski *et al.*, 2020). The participation of phenolic compounds and flavonoids from *Elaeis guineensis* in the biosynthesis of gold nanoparticles was demonstrated by the reduction of the content of these metabolites quantified by Ahmad *et al.* (2019). Quercetin was also an effective reductant agent in the green synthesis of silver and gold nanoparticles (Karuvantevida *et al.*, 2022). Then, it is possible to relate the occurrence of these two classes of compounds to the capping and reducing action of the extract.

It could be observed an absorption band in 280 nm in the UV-VIS spectrum (Fig. 1), which is related to the flavonoids (Tošović and Marković, 2017) present the extract (Fig. A1 of the Appendix). Besides, a strong absorption band at 423 nm was observed for AgNPs-MI solution, which can be attributed to the surface plasmon resonance phenomena that is typical for AgNPs. An absorption band around 400 nm also characterizes spherical nanoparticles (Grzygorczyk *et al.*, 2021; Tošović and Marković, 2017).
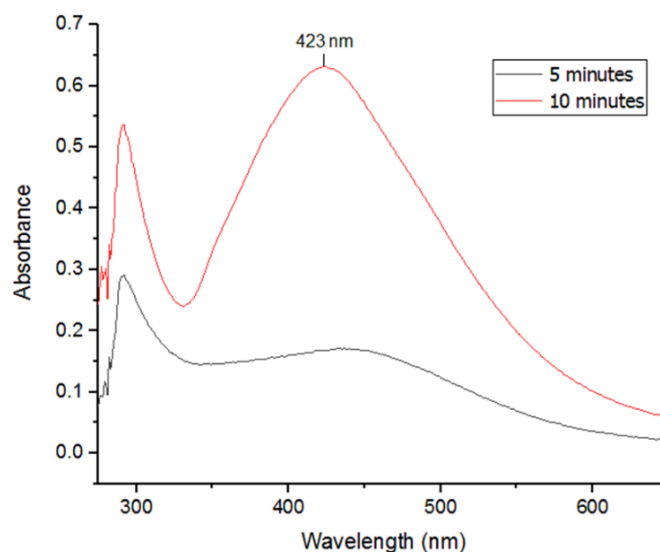

Figure 1. UV-VIS spectra of a freshly-prepared AgNPs-MI suspension after 5 min (—) and 10 min (—) of reaction.

By using DLS, it was verified that a bimodal size distribution was found for AgNPs-MI, corresponding to the average hydrodynamic diameters of 4.0 to 342.0 nm (Fig. A2a of the Appendix). The large particle sizes observed by using this technique can be explained by the fact that DLS measurements provides hydrodynamic sizes (Bojko *et al.*, 2020). In consequence, the diameter includes the molecules that stabilize the nanoparticles, which leads to an observation of a value higher than the real (Lin *et al.*, 2013). Zeta potential of the nanocomposite suspension was found to be –21.8 mV (Fig. A2b of the Appendix), which indicates that the nanoparticles were suitably capped with anionic extract metabolites. Despite the found value had been lower than typical potential range of stable colloids (–30.0 mV to +30.0 mV) (Efavi *et al.*, 2022), some research reported stable AgNPs with similar zeta potential values (Ahmad *et al.*, 2016a). Thus, such observations have proved the efficiency of *M. Ilicifolia* as a capping agent. The polydispersion index (PDI) was calculated for verifying the homogeneity in the AgNPs-MI size. The sample analyzed showed PDI = 0.516. Thus, the AgNPs-MI are polydispersive, since the PDI near to zero indicates monodispersive nanoparticles and PDI = 1 indicates a big variation in the particle size (Lin *et al.*, 2013).

The images obtained by FEG-MEV analysis confirm that the AgNPs-MI show homogeneous size and spherical shape, with just few aggregates observed (Figs. 2a–d). Besides, the high yield of the biosynthesis could be considered due to the high amount of AgNPs-MI detected (Fig. 2a), which showed particles sizes in the range of 20–80 nm.
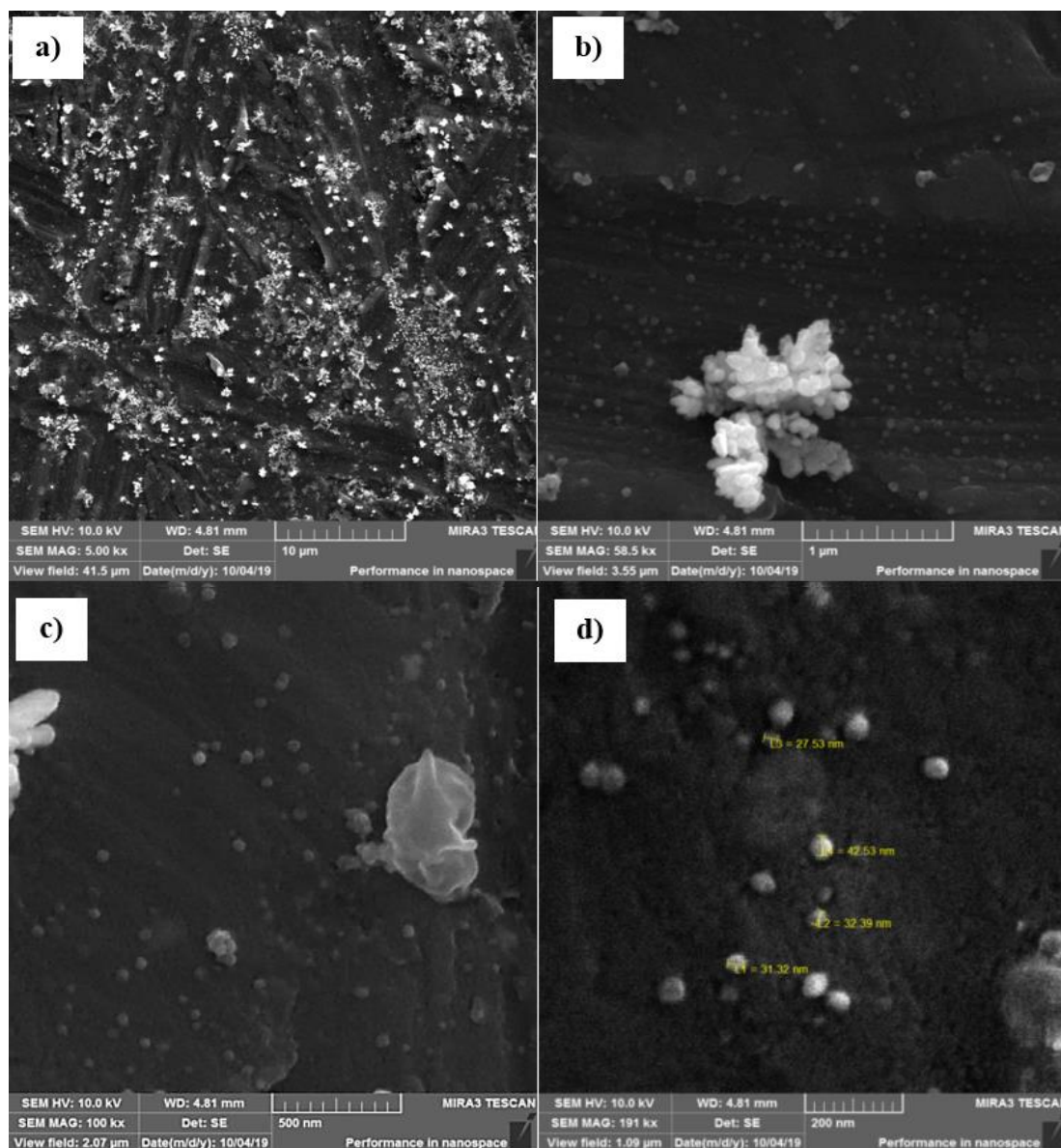
Figure 2. FEG-MEV Images obtained by analysis of AgNPs-MI with different magnifications **(a)** 5,00 kx; **(b)** 58,5 kx; **(c)** 100 kx, and **(d)** 191 kx.

Analyzing the AgNPs-MI FTIR spectra (Fig. 3), it is possible to observe that the bands intensity at 1641 (C=O stretching) and 3418 cm^{-1} (OH stretching) was decreased. This fact is probably related to their participation in the stabilization of the AgNPs. The absorption bands at 2848 (COO-H stretching) 1776 (C=O stretching) and 823 cm^{-1} (C-O stretching), were observed and they can be attributed to carboxylic groups (Haddad *et al.*, 2014). These bands suggest the occurrence of flavonoids and phenolic compounds from *M. ilicifolia* extract, which interacts with AgNPs through the electron donors oxygen atoms. Those biomolecules can be adsorbed on the metal ions surface, which is observed by the decreasing in the intensity of the bands observed. The band at 1776 cm^{-1} evidences the influence

of the extracts in the formation of the AgNPs, considering the oxidation of this material and, in consequence, the reduction of Ag$^+$ ions.

The AgNPs-MI were also analyzed by Raman spectroscopy (Fig. A3 of the Appendix). The Raman spectrum displayed a band at 236 cm^{-1} related to the vibration of stretching Ag-O bond (Barbosa, 2007). This band can be related to the interaction between Ag and carboxylate groups of the molecules of the extract, attached to the AgNPs-MI surface, which contribute to this stabilization. The peaks at 1365 e 1522 cm^{-1} were, respectively, attributed to the symmetric and asymmetric vibrations of C=O of carboxylate group (Barbosa, 2007).
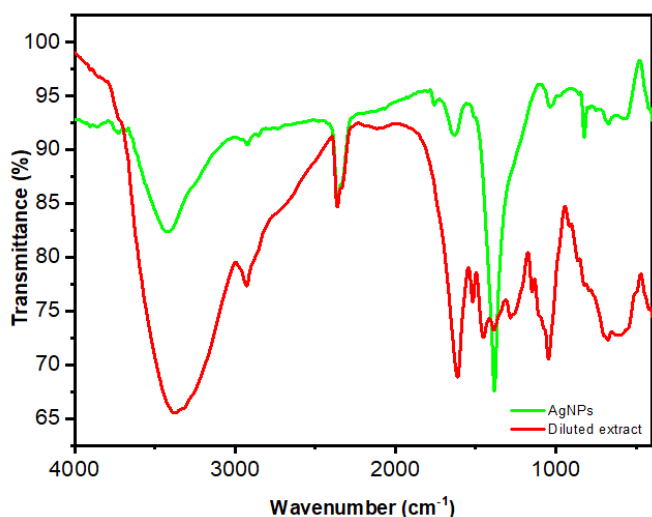
Figure 3. FTIR spectra of *M. ilicifolia* (—diluted aqueous extract) and (—AgNPs-MI).

3.2 Electrochemical characterization of GCPE, GCPE/MI and GCPE/AgNPs-MI

The electron transfer properties of bare GCPE, GCPE/MI and GCPE/AgNPs-MI were evaluated by CV and EIS techniques. The studies were carried out in the presence of 10.0 mmol L^{-1} $K_4Fe(CN)_6/K_3Fe(CN)_6$ as a redox probe, with 0.15 mol L^{-1} PBS buffer solution as supporting electrolyte, pH = 6.5. Analyzing the cyclic voltammograms (Fig. 4) and the data reported in the Table 1, it is possible to verify that both electrodes showed current peaks for the typical redox process of the electrochemical probe ($Fe(CN)_6^{4-} \rightleftharpoons Fe(CN)_6^{3-}$). However, GCPE/AgNPs-MI showed higher anodic peak (I_{pa}) and cathodic peak (I_{pc}) currents for both processes than bare GCPE. GCPE/AgNPs-MI also showed low peak potential separation values (ΔE_p). This suggest that the electronic transfer kinetic is more effective and show higher reversibility (C. Brett and A. Brett, 1993) when compared to bare GCPE.
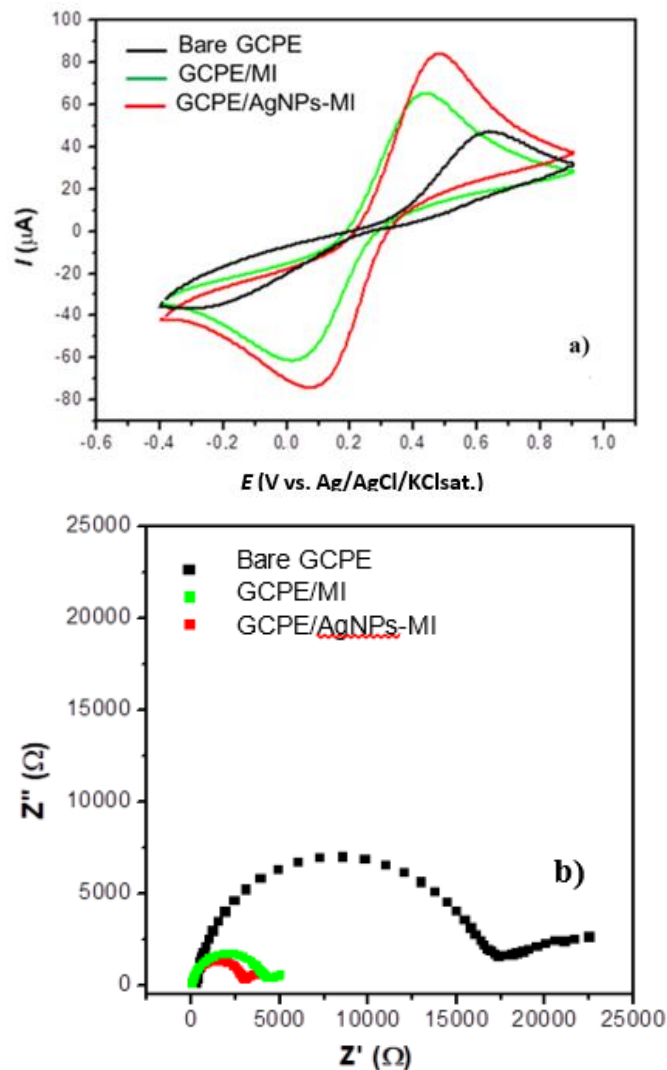

Figure 4. **(a)** Cyclic voltammograms (scan rate = 50.0 mV s^{-1}) and **(b)** electrochemical impedance spectra (Nyquist plots) of GCPE/AgNPs-MI, GCPE/MI and bare CPE (open circuit potential; frequency range: 5 kHz to 25 mHz; amplitude: 10 mV), in 0.15 mol L^{-1} PBS buffer solution (pH 6.5) containing 10.0 mmol L^{-1} $K_4Fe(CN)_6/K_3Fe(CN)_6$.

Table 1. I_{pa}, I_{pc}, ΔE_p and R_{ct} values obtained for bare GCPE, GCPE/MI and GCPE/AgNPs-MI.

Electrode	I_{pa} (μA)	- I_{pc} (μA)	E_{pa} (mV)	E_{pc} (mV)	ΔE_p	R_{ct} (Ω)
Bare GCPE	26.19	18.40	638	233	405	17389.99
GCPE/MI	58.27	49.50	431	19	412	4102.10
GCPE/AgNPs-MI 50 μL	71.64	65.13	477	81	396	2863.30

Since the diameter of the semicircle is related to the electronic transfer resistance (R_{ct}) (C. Brett and A. Brett, 1993; Van Der Horst *et al.*, 2015) it was observed that this parameter for bare GCPE was higher than for GCPE/AgNPs-MI and GCPE/MI. This suggests that GCPE/MI and GCPE/AgNPs-MI facilitates the electron

transfer process in electrode-solution interface when compared to the bare GCPE. These results are in accordance with that obtained by CV. Besides, they can be better understood when evaluated together with the R_{ct} values obtained in each situation (Table 2). The higher current values, lower ΔE_p and lower R_{ct} exhibited

by GCPE/AgNPs-MI can be attributed to the characteristics of AgNPs, such as high conductivity and big surface area (C. Brett and A. Brett, 1993). This suggest that the modification of the electrode with the nanocomposite obtained in this study is an advantage for its application as an electrochemical sensor.

In order to evaluate the influence in the amount of AgNPs-MI added in the GCPE electrochemical response, different volumes of AgNPs-MI (10, 25, 50, 75 and 100 µL) were added to 50.0 mg of powder glassy carbon. The electrodes response was analyzed in the presence of $[Fe(CN)_6]^{3-}/[Fe(CN)_6]^{4-}$ 10 mmol L^{-1} in PBS buffer 0.15 mol L^{-1} as electrolyte support.

Table 2. I_{pa}, I_{pc}, ΔE_p and R_{ct} values of bare GCPE and GCPE/AgNPs-MI in different volumes.

Electrode	I_{pa} (µA)	- I_{pc} (µA)	E_{pa} (mV)	E_{pc} (mV)	ΔE_p	R_{ct} (Ω)
Bare GCPE	26.19	18.40	638	233	405	17389.99
GCPE/AgNPs-MI 10 µL	72.73	64.60	481	33	448	3910.00
GCPE /AgNPs-MI 25 µL	62.00	61.16	485	58	427	4991.30
GCPE /AgNPs-MI 50 µL	**71.64**	**65.13**	**477**	**81**	**396**	**2863.30**
GCPE /AgNPs-MI 75 µL	49.4	41.52	514	5	509	6909.80
GCPE /AgNPs-MI 100 µL	64.18	56.02	415	94	321	3490.40

The anodic peak current (I_{pa}) was decreased until 25 µL, and, after this, a higher I_{pa} was observed with 50 µL (Fig. 5); then, the current decreased again. When GCPE/AgNPs-MI 10 µL and GCPE/AgNPs-MI 50 µL were compared, it was possible to verify that both showed similar current responses. However, the GCPE/AgNPs-MI with 50 µL exhibited a low ΔE_p as well as a lower R_{ct} values, suggesting that, for those conditions, the charge transfer process in the electrode-solution interface is fast. Moreover, it shows higher reversibility for the process (Van Der Horst *et al.*, 2015), when compared with GCPE/AgNPs-MI obtained with 10 µL. Hence, 50 µL of AgNPs-MI was chosen as the amount for the preparation of the modified CPE electrodes.
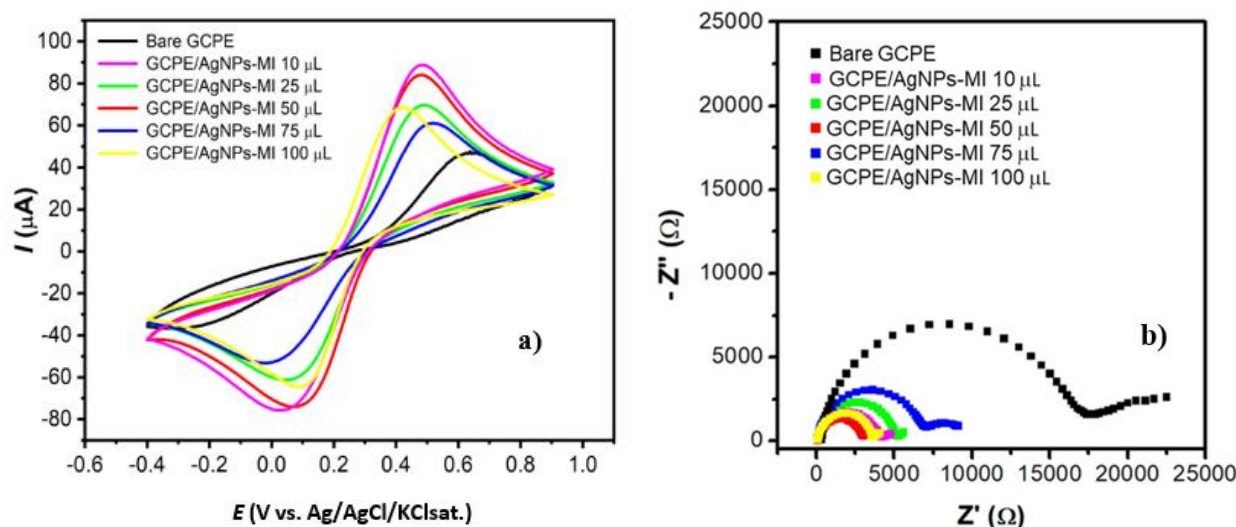

Figure 5. **(a)** Cyclic voltammograms and **(b)** electrochemical impedance spectra of GCPE/AgNPs-MI and bare GCPE, in an equimolar solution of $K_4Fe(CN)_6/K_3Fe(CN)_6$ 0.010 mol L^{-1} in PBS buffer solution 0.15 mol L^{-1} (pH 6.5).

3.3 Effect of pH

The pH of the supporting electrolyte is an important parameter for the analytical performance of the sensor. It can influence in the electrochemical response of the device during the detection of the analyte (Lima *et al.*, 2018). Since there are protons involved in the DA electrooxidation mechanism, the effect of pH of the supporting electrolyte on the electrochemical response of GCPE/AgNPs-MI (50 µL) for 1×10^{-2} mol L^{-1} of DA was evaluated. The voltammograms were obtained in 0.04 mol L^{-1} BR buffer with different pH values (pH 2.0–7.0) by employing the SWV technique (Fig. 6).
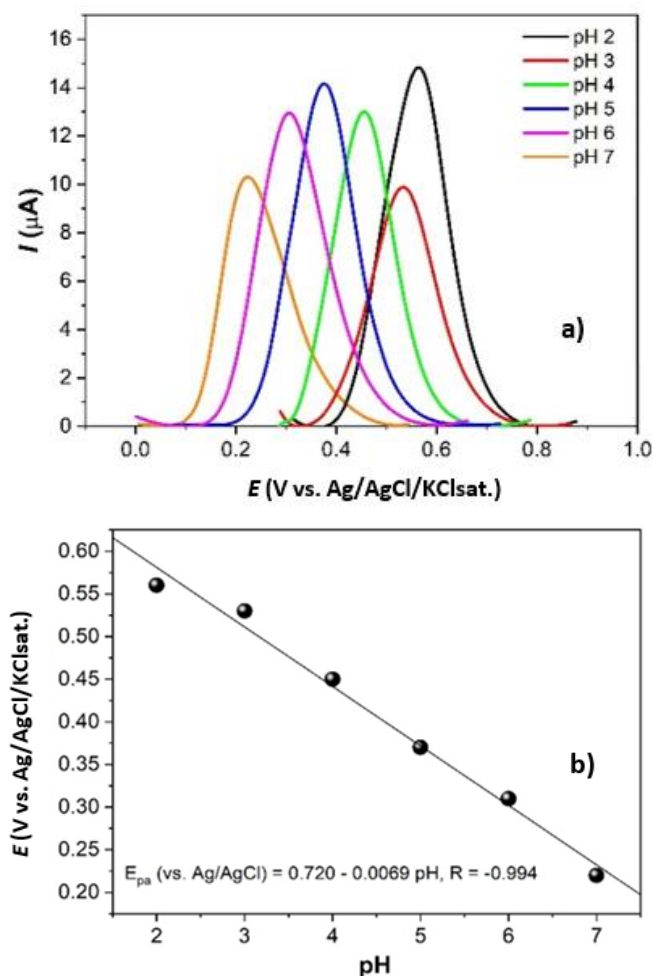
Figure 6. Effect of pH in the electrochemical response of DA. **(a)** Square wave voltammograms of 1.0×10^{-2} mol L^{-1} of DA on GCPE/AgNPs-MI in BR buffer 0.04 mol L^{-1}, at pH in the range of 2.0 to 7.0. **(b)** Relationship between de E_{pa} and pH obtained from the voltamograms.

The effect of pH in the current and potential values was also evaluated. The DA peak potential shifted negatively with the increase of the pH values (Fig. 6), since the electrooxidation of DA involves 2 protons and 2 electrons, leading to the DA quinone, which can be reduced in the reverse process (Sakthivel *et al.*, 2017). A linear relationship was verified between the anodic peak potential and the pH medium according to the following linear regression equation: (E_{pa} (vs. Ag/AgCl) = 0.720–0.069 pH, R = 0.994). The slope obtained was of −69.0 mV pH^{-1}, which was close to the theoretical Nernstian value of −59.0 mV pH^{-1}, suggesting that the number of electrons and protons transferred in the electrode reaction is the same (Lima *et al.*, 2018).

DA shows voltammetric response on the GCPE/AgNPs-MI for all pH range studied, and the highest current value was obtained in pH 2.0. However,

pH 7.0 was chosen for further analysis, because a biological application for the sensor is intended.

3.4 Influence of scan rate

In order to determine the mechanism of mass transport in the redox reaction of DA on the GCPE/AgNPs-MI, the influence of the scan rate on the voltammetric profile was analyzed, by recording cyclic voltammograms for 1.0×10^{-2} mol L^{-1} of DA (fixed concentration) in the range of 10–100 mV s^{-1}. The supporting electrolyte was BR buffer 0.04 mol L^{-1} at pH 7.0. A linear relationship was noticed in the plot of $\log(I_p)$ vs. $\log(\nu)$, corresponding to the equation $\log(I_{pa}) = 0.270 + 0.373 \log(\nu)$; R = 0.985 (Fig. 7).The slope value of 0.37 is close to 0.50, which is the theoretically expected value for a totally diffusion-controlled process. Therefore, it was concluded that the electrochemical oxidation of DA on GCPE/AgNPs-MI is mostly governed by diffusion (Lima *et al.*, 2018).
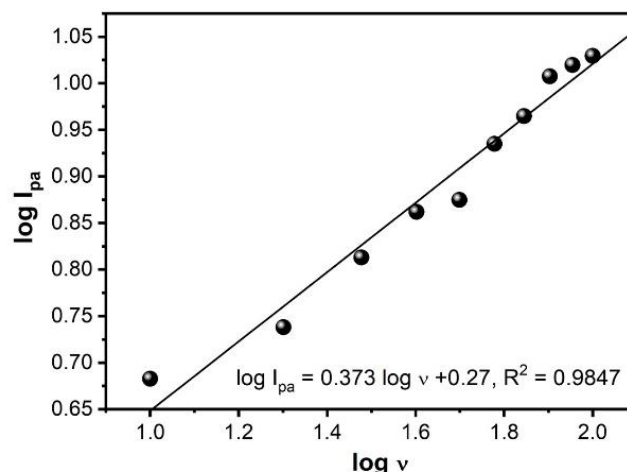

Figure 7. Relationship of $\log I_{pa}$ vs. $\log \nu$ for DA.

3.5 Analytical curves

DA quantitative analysis employing the GCPE/AgNPs-MI were recorded by SWV (Fig. 8a). Analytical curves (Fig. 8b) were constructed under the optimum conditions in the range of 30 to 90 µmol L^{-1} of DA, by using 0.04 mol L^{-1} BR buffer solution as supporting electrolyte at pH 7.0. The regression equation obtained by the linear regression of the average of three analytical curves and the correlation coefficient are shown in Table 3.

The analytical curves indicated a linear increase of I_{pa} value with the increase of DA concentration in the concentration range studied. From this curve, it was

possible to calculate the detection (LOD) and the quantification (LOQ) limits for the electrode evaluated. LOD and LOQ values were calculated as recommended by ANVISA (2003) and ICH (2005) guidelines: LOD = 3 SD/b and LOQ = 10 SD/b, where SD is the standard deviation of the intercepts (n = 3) and b is the slope of the analytical curve. The obtained results are shown in Table 3, along with the linear range, regression equation, standard error and correlation coefficient of each electrode.
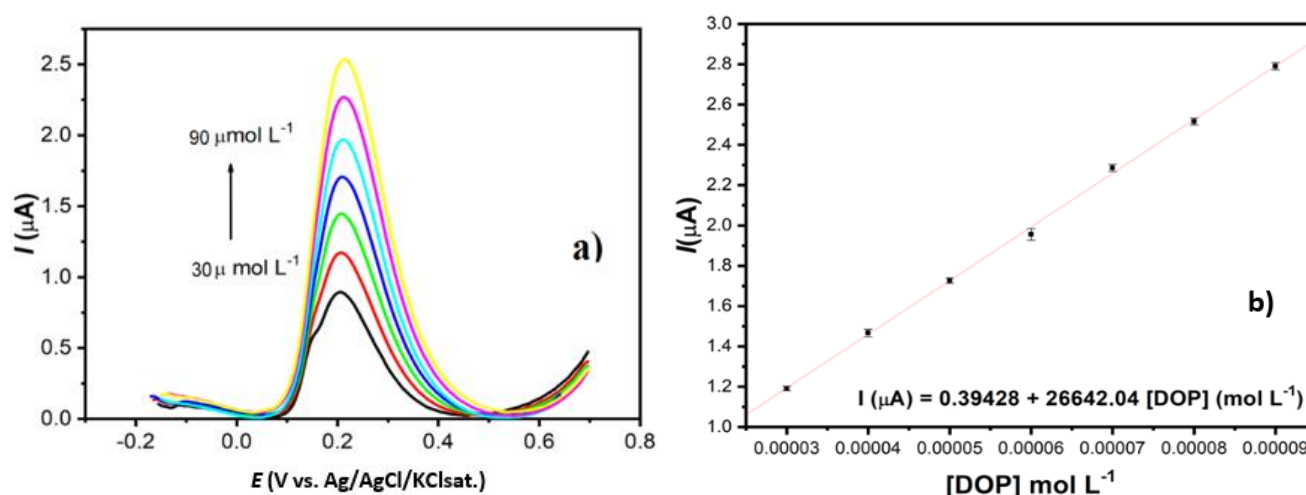

Figure 8. DA quantitative analysis using the GCPE/AgNPs-MI. **(a)** Square wave voltammograms obtained in the range of 30 to 90 µmol L^{-1} of DA, on GCPE/AgNPs-MI, in BR buffer 0.04 mol L^{-1} at pH 7.0, with a = 90 mV, f = 100 Hz e ΔEs = 8 mV. **(b)** Analytical curves obtained for GCPE/AgNPs-MI (average of three measurements).

Table 3. Analytical parameters obtained from the linear regression curves of GCPE/AgNPs-MI for DA determination by using SWV.

Parameter	GCPE/AgNPs-MI
Linear range (µmol L^{-1})	30.0 – 90.0
Regression equation	I (µA) = 0.39428 + 26642.04 [DOP] (µmol L^{-1})
Correlation coefficient	0.999
LOD (µmol L^{-1})	0.52
LOQ (µmol L^{-1})	1.74

Considering the low LOD (0.52 µmol L^{-1}) and LOQ (1.74 µmol L^{-1}) values obtained, it is possible to verify the good sensitivity of the modified electrode. Thus, those detection and quantification limits can be considered satisfactory for determination of DA in biological samples and pharmaceutical formulations. Besides, the values described in this work are comparable with other electrochemical methods previously reported in the literature (Table 4).

Table 4. Comparison of LOD values for DA detection using electrochemical and other analytical methods.

Technique	Working Electrode	LOD (µmol L^{-1})	Reference
DPV	Glassy carbon electrodes modified with CdTe quantum dots	0.30	Yu *et al*. (2018)
SWV	Gold electrode modified with a nanostructure of polypyrrole-mesoporous molecular silica film	0.70	Zablocka *et al*. (2019)
CV	AuNPs-modified screen-printed carbon electrode	0.20	Chelly *et al*. (2021)
CV	Glassy carbon electrodes modified with AgNPs using *Ziziphus mauritiana* extract	0.10	Memon *et al*. (2021)
SWV	CPE modified with iron oxide (Fe$_2$O$_3$) nanoparticle	0.79	Vinay and Nayaka (2019)
DPV	Electrode printed in graphite screen modified by nanocomposite film	0.86	Selvolini *et al*. (2019)
SWV	**GCPE/AgNPs-MI**	**0.52**	**This work**

DPV= differential pulse voltammetry.

3.6 Accuracy, repeatability and recover assays

The accuracy of GCPE/AgNPs-MI for the determination of DA was evaluated by determination of the repeatability levels (intraday precision) of the voltammetric response generated by the sensor in the presence of the analyte, as well as considering the reproducibility level of preparation of the modified electrode. For this purpose, SWV measurements (n = 10) were carried out in the presence of 1.0×10^{-2} mol L^{-1} of the analyte, in the same day, and the results were expressed in terms of relative standard deviation (%RSD) between the found concentrations. For the evaluation of reproducibility, five independent GCPE/AgNPs-MI were prepared (n = 5) and tested in the same conditions, as mentioned above.

The results obtained for the accuracy and precision studies were expressed in terms of %RSD between the I_{pa} obtained. It was observed that the GCPE/AgNPs-MI presented satisfactory repeatability (%RSD = 3.66) and precision (%RSD = 4.47) levels for the determination of DA, since %RSD values were lower than 5.00%, that are in good agreement with the ANVISA (2003) and

ICH (2005) guidelines. In order to verify the amount of DA, which could be quantified by GCPE/AgNPs-MI, assays of DA recovery were done by SWV, using the supporting electrolyte BR buffer 0.04 mol L^{-1} at pH 7.0).

These studies were performed by using the linear regression of the analytical curves for GCPE/AgNPs-MI (Fig. 8b) and the results obtained reveal the possibility of using the sensor in the determination of DA in real samples. For this, aliquots of DA (30, 50 and 70 µmol L^{-1}) stock solution were added to the electrochemical cell. For each addition, the current value was registered. After, the concentration of DA was obtained by the linear regression I (µA) = 0.39428 + 26642.04 [DA]. The experiments were carried out in triplicate (n = 3) by the standard addition method, and the results were expressed as percent recovery, as shown in Table 5. It could be observed that the percent recoveries were obtained in three different amounts of DA indicating that the matrix does not significantly affect the response of the modified electrode for DA detection. Therefore, these results clearly show that GCPE/AgNPs-MI may be efficiently applied for the quantification of DA in real samples, with good accuracy and precision.

Table 5. Results for the recovery of DA in injection with GCPE/AgNPs-MI by SWV.

Added (µmol L^{-1})	Found (µmol L^{-1})	(RSD%)	Recovery (%)
30.00	30.88 ± 0.07	2.22	102.93
50.00	50.9 ± 0.3	2.90	101.82
70.00	70.7 ± 0.4	3.05	101.04

4. Conclusions

In this review, recent literature on UV-blocking textiles have been reported to give an overview of their importance and prospects in sun-protective methods. UV-protective compounds incorporated, anchored, or coated textile fibers compose a useful class of UV-blocking materials for the development of smart fabrics as proved by the large number of scientific publications in the last years. Different UV-protective compounds, mainly TiO$_2$ and ZnO, are used to improve UV-blocking ability of fabrics and, often, they also impart to additional fabric properties, e.g., antibacterial, and self-cleaning activities. Analyzing from spectroscopic point of view, the elucidation of UV-blocking mechanisms gives an important information about electronic structure and optical properties of UV-protective textiles; therefore, it can be more investigated and discussed in the literature. A remarkable point is the reduced number of scientific papers that reported the use of organic filters in smart fabrics although these UV-protective compounds have

high UV absorption capacity and, depending on their molecular structure, can interact to fiber surface without the presence of cross-linker compounds. UPF is a good parameter to indicate the UV-blocking ability of UV-protective compound-containing smart fabrics, however, some aspects must be considered in the analyses and interpretation of UPF results. Among them, (i) the amount of the UV-protective compound per textile area, (ii) textile thickness, and (iii) textile properties changed by the incorporation, coating and/or anchorage with UV-protective compounds, e.g., textile roughness. In this perspective, new scientific studies need to be undertaken to know the effective contribution of UV-protective compounds in the UPF values. Considering the growing requirement for simple, cheap, and practical sun-protective products, UV-blocking textiles are one of the best alternatives. Thus, scientific research in the field of smart fabric and/or UV-blocking textile, especially UV-protective compounds incorporated, anchored, or coated textile fibers, must be encourage in order to promote new

insights in sun-protective clothing and future applications of multifunctional textiles.

Authors' contribution

Conceptualization: Humacayo, F. S.; Magalhães, C. G.
Data curation: Humacayo, F. S.; Espinoza, J. T.; Lopes, L. C.
Formal Analysis: Magalhães, C. G.; Paula, J. F. P.; Pessoa, C. A.
Funding acquisition: Not applicable.
Investigation: Humacayo, F. S.
Methodology: Humacayo, F. S.; Espinoza, J. T.; Lopes, L. C.
Project administration: Magalhães, C. G.; Paula, J. F. P.; Pessoa, C. A.
Resources: Not applicable.
Software: Not applicable.
Supervision: Magalhães, C. G.; Paula, J. F. P.; Pessoa, C. A.
Validation: Magalhães, C. G.; Paula, J. F. P.; Pessoa, C. A.
Visualization: Magalhães, C. G.; Paula, J. F. P.; Pessoa, C. A.
Writing – original draft: Humacayo, F. S.; Espinoza, J. T.; Lopes, L. C.
Writing – review & editing: Magalhães, C. G.; Paula, J. F. P.; Pessoa, C. A.

Data availability statement

The data will be available upon request.

Funding

Acknowledgments

References

Agência Nacional de Vigilância Sanitária (ANVISA), Guia para Validação de Métodos Analíticos e Bioanalíticos. Ministério da Saúde, Brasil (Resolução – RE nº 899, de 29 de maio de 2003), 2003. https://bvsms.saude.gov.br/bvs/saudelegis/anvisa/2003/res0899_29_05_2003.html (accessed 2021-03-21).

Ahmad, A.; Syed, F.; Imran, M.; Khan, A. U.; Tahir, K.; Khan, Z. U. H.; Yuan, Q. Phytosynthesis and antileishmanial activity of gold nanoparticles by Maytenus royleanus. J. Food Biochem. 2016a, 40 (4), 420–427. https://doi.org/10.1111/jfbc.12232

Ahmad, A.; Wei, Y.; Syed, F.; Tahir, K.; Taj, R.; Khan, A. U.; Hameed, M. U.; Yuan, Q. Amphotericin B-conjugated biogenic silver nanoparticles as an innovative strategy for fungal infections. *Microb. Pathog*. **2016b** *99*, 271–281. https://doi.org/10.1016/j.micpath.2016.08.031

Ahmad, T.; Bustam, M. A.; Irfan, M.; Moniruzzaman, M.; Asghar, H. M. A.; Bhattacharjee, S. Mechanistic investigation of phytochemicals involved in green synthesis of gold nanoparticles using aqueous *Elaeis guineensis* leaves extract: Role of phenolic compounds and flavonoids. *Biotech. Appl. Biochem.* **2019**, *66* (4), 698–708. https://doi.org/10.1002/bab.1787

Barbosa, L. C. A. Espectroscopia no Infravermelho na Caracterização de Compostos Orgânicos, Editora UFV, 2007.

Bastos-Arrieta, J.; Florido, A.; Pérez-Ràfols, C.; Serrano, N.; Fiol, N.; Poch, J.; Villaescusa, I. Green Synthesis of Ag Nanoparticles Using Grape Stalk Waste Extract for the Modification of Screen-Printed Electrodes. *Nanomaterials.* **2018**, *8* (11), 946. https://doi.org/10.3390/nano8110946

Blum, S. A.; Zahrebelnei, F.; Nagata, N.; Zucolotto, V.; Mattoso, L. H. C.; Pessoa, C. A.; K. Wohnrath, K. Experimental Design to Enhance Dopamine Electrochemical Detection Using Carbon Paste Electrodes. *Braz. J. Analytical Chem*. **2021**, *8* (32), 178–197. https://doi.org/10.30744/brjac.2179-3425.AR-31-2021

Bojko, L.; Jonge, G.; Lima, D.; Lopes, L. C.; Viana, A. G.; Garcia, J. R.; Pessôa, C. A.; Wohnrath, K.; Inaba, J. Porphyran-capped silver nanoparticles as a promising antibacterial agent and electrode modifier for 5-fluorouracil electroanalysis. *Carb. Res.* **2020**, *498*, 108193. https://doi.org/10.1016/j.carres.2020.108193

Brett, C. M. A.; Brett, A. M. O. Electrochemistry: Principles, Methods, and Applications, Oxford University Press, 1993.

Broli, N.; Vallja, L.; Shehu, A.; Vasjari, M. Determination of catechol in extract of tea using carbon paste electrode modified with banana tissue. *J. Food Process Preserv.* **2019**, *43* (6), e13838. https://doi.org/10.1111/jfpp.13838

Chelly, M.; Chelly, S.; Zribi, R.; Bouaziz-Ketata, H.; Gdoura, R.; Lavanya, N.; Veerapandi, G.; Sekar, C.; Neri, G. Synthesis of silver and gold nanoparticles from *Rumex roseus* plant extract and their application in electrochemical sensors. *Nanomaterials*. **2021**, *11* (3), 739. https://doi.org/10.3390/nano11030739

Efavi, J. K.; Nyankson, E.; Kyeremeh, K.; Manu, G. P.; Asare, K.; Yeboah, N. Monodispersed AgNPs Synthesized from the nanofactories of *Theobroma cacao* (cocoa) leaves and pod

husk and their antimicrobial activity. *Int. J. Biomat.* **2022**, *2022*, 4106558. https://doi.org/10.1155/2022/4106558

Grzygorczyk, S.; Ezpinoza, J. T.; Paula, J. F. P.; Boscardin, P. M. D.; Nunes, D. S.; Sandri, M. C. M.; Magalhães, C. G. Evaluation of the biotechnological potential of *Monteverdia salicifolia* (Mart ex. Reissek) Biral. *Orbital: Electron. J. Chem.* **2021**, *13* (2), 140–144. https://doi.org/10.17807/orbital.v13i2.1545

Haddad, Z.; Abid, C.; Oztop, H. F.; Mataoui, A. A review on how the researchers prepare their nanofluids. *Int. J. Therm. Sci.* **2014**, *76*, 168–189. https://doi.org/10.1016/j.ijthermalsci.2013.08.010

Huq, A.; Ashrafudoulla, M.; Rahman, M.; Balusamy, R.; Akter, S. Green synthesis and potential antibacterial applications of bioactive silver nanoparticles: A review. *Polymers.* **2022**, *14* (4), 742–764. https://doi.org/10.3390/polym14040742

International Conference on Harmonisation (ICH). Harmonised Tripartite Guideline. Validation of Analytical Procedures: Text and Methodology Q2 (R1). ICH Expert Working Group, 2005. https://database.ich.org/sites/default/files/Q2%28R1%29%20 Guideline.pdf (accessed 2019-05-22).

Jadoun, S.; Arif, R.; Jangid, N. K.; Meena, R. K. Green synthesis of nanoparticles using plant extracts: A review. *Environ. Chem. Lett*. **2021**, *19* (1), 355–374. https://doi.org/10.1007/s10311-020-01074-x

Karuvantevida, N.; Razia, M.; Bhuvaneshwar, R.; Sathishkumar, G.; Prabukumar, S.; Sivaramakrishnan, S. Bioactive flavonoid used as a stabilizing agent of mono and bimetallic nanomaterials for multifunctional activities. *J. Pure Appl. Microbiol.* **2022**, *16* (3), 1652–1662. https://doi.org/10.22207/JPAM.16.3.03

Lima, D.; Calaça, G. N.; Viana, A. G.; Pessôa, C. A. Porphyran-capped gold nanoparticles modified carbon paste electrode: A simple and efficient electrochemical sensor for the sensitive determination of 5-fluorouracil. *Appl. Surf. Sci.* **2018**, *427* (Part B), 742–753. https://doi.org/10.1016/j.apsusc.2017.08.228

Lima Filho, M. M. S.; Correa, A. A.; Silva, F. D. C.; Carvalho, F. A. O.; Mascaro, L. H.; Oliveira, T. M. B. F. A glassy carbon electrode modified with silver nanoparticles and functionalized multi-walled carbon nanotubes for voltammetric determination of the illicit growth promoter dienestrol in animal urine. *Microchim. Acta.* **2019**, *186*, 525. https://doi.org/10.1007/s00604-019-3645-9

Lin, J.; Yeap, S. P.; Che, H. X.; Low, S. C. Characterization of magnetic nanoparticle by dynamic light scattering. *Nanoscale Res. Lett.* **2013**, *8*, 381. https://doi.org/10.1186/1556-276X-8-381

Memon, R.; Memon, A. A.; Nafady, A.; Sirajuddin; Sherazi, S. T. H.; Balouch, A.; Memon, K.; Brohi, N. A.; Najeeb, A. Electrochemical sensing of dopamine via bio-assisted synthesized silver nanoparticles. *Int. Nano Lett.* **2021**, *11* (3), 263–271. https://doi.org/10.1007/s40089-021-00339-9

Orlowski, P.; Zmigrodzka, M.; Tomaszewska, E.; Ranoszek-Soliwoda, K.; Pajak, B.; Slonska, A.; Cymerys, J.; Celichowski, G.; Grobelny, J.; Krzyzowska, M. Polyphenol-conjugated bimetallic Au@AgNPs for improved wound healing. *Int. J. Nanomed.* **2020**, *15*, 4969–4990. https://doi.org/10.2147/IJN.S252027

Périco, L. L.; Rodrigues, V. P.; Almeida, L. F. R.; Fortuna-Perez, A. P.; Vilegas, W.; Hiruma-Lima, C. A. *Maytenus ilicifolia* Mart. ex Reissek. In *Medicinal and Aromatic Plants of South America*. Albuquerque, U., Patil, U., Máthé, Á, Eds.; Springer, 2018; Vol. 5, 323–335. https://doi.org/10.1007/978-94-024-1552-0_29

Relação Nacional de Plantas Medicinais de Interesse ao SUS (RENISUS). Espécies vegetais. Ministério da Saúde, 2009. https://www.gov.br/saude/pt-br/composicao/sctie/daf/pnpmf/ppnpmf/arquivos/2014/renisu s.pdf (accessed 2022-10-06).

Sakthivel, R.; Dhanalakshmi, S.; Chen, S.-M.; Chen, T.-W.; Selvam, V.; Ramaraj, S. K.; Weng, W.-H.; Leung, W.-H. A novel flakes-like structure of molybdenum disulphide modified glassy carbon electrode for the efficient electrochemical detection of dopamine. *Int. J. Electrochem. Sci.* **2017**, *12*, 9288–9300. https://doi.org/10.20964/2017.10.71

Selvolini, G.; Lazzarini, C.; Marrazza, G. Electrochemical nanocomposite single-use sensor for dopamine detection. *Sensors*. **2019**, *19* (14), 3097. https://doi.org/10.3390/s19143097

Tabach, R.; Duarte-Almeida, J. M.; Carlini, E. A. Pharmacological and toxicological study of *Maytenus ilicifolia* leaf extract. Part II—Clinical Study (Phase I). *Phytother. Res.* **2017**, *31* (6), 921–926. https://doi.org/10.1002/ptr.5816

Tošović, J.; Marković, S. Reproduction and interpretation of the UV–vis spectra of some flavonoids. *Chem. Pap*. **2017**, *71* (3), 543–552. https://doi.org/10.1007/s11696-016-0002-x

Van Der Horst, C.; Silwana, B.; Iwuoha, E.; Somerset, V. Bismuth–silver bimetallic nanosensor application for the voltammetric analysis of dust and soil samples. *J. Electroanal. Chem.* **2015**, *752*, 1–11. https://doi.org/10.1016/j.jelechem.2015.06.001

Vinay, M. M.; Nayaka, Y. A. Iron oxide (Fe_2O_3) nanoparticles modified carbon paste electrode as an advanced material for electrochemical investigation of paracetamol and dopamine. *J. Sci.-Adv. Mater. Dev.* **2019**, *4* (3), 442–450. https://doi.org/10.1016/j.jsamd.2019.07.006

Yu, H.-W.; Zhang, Z.; Jiang, J.-H.; Pan, H.-Z.; Chang, D. Simple strategy for sensitive detection of dopamine using CdTe QDs modified glassy carbon electrode. *J. Clin. Lab. Anal.* **2018**, *32*, e22320. https://doi.org/10.1002/jcla.22320

Zablocka, I.; Wysocka-Zolopa, M.; Winkler, K. Electrochemical detection of dopamine at a gold electrode modified with a polypyrrole–mesoporous silica molecular sieves (MCM-48) film. *Int. J. Mol. Sci.* **2019**, *20* (1), 111. https://doi.org/10.3390/ijms20010111

Zamarchi, F.; Vieira, I. C. Determination of paracetamol using a sensor based on green synthesis of silver nanoparticles in plant extract. *J. Pharm. Biomed. Anal.* **2021**, *196*, 113912. https://doi.org/10.1016/j.jpba.2021.113912

Zhang, L.; Ji, M.-Y.; Qiu, B.; Li, Q.-Y.; Zhang, K.-Y.; Liu, J.-C.; Dang, L.-S.; Li, M.-H. Phytochemicals and biological activities of species from the genus *Maytenus*. *Med. Chem. Res.* **2020**, *29* (4), 575–606. https://doi.org/10.1007/s00044-020-02509-4
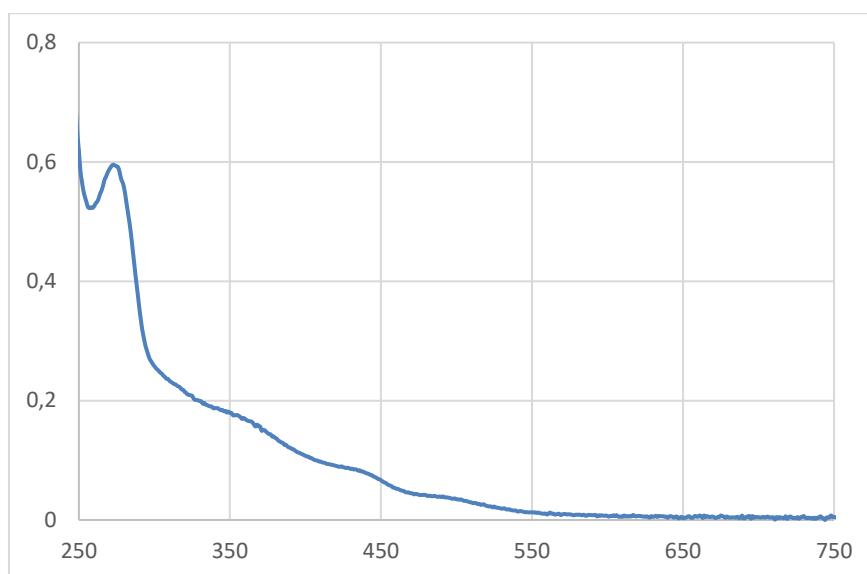
Appendix

Figure A1. UV-Vis spectrum of aqueous extract of the leaves from *M. ilicifolia*.
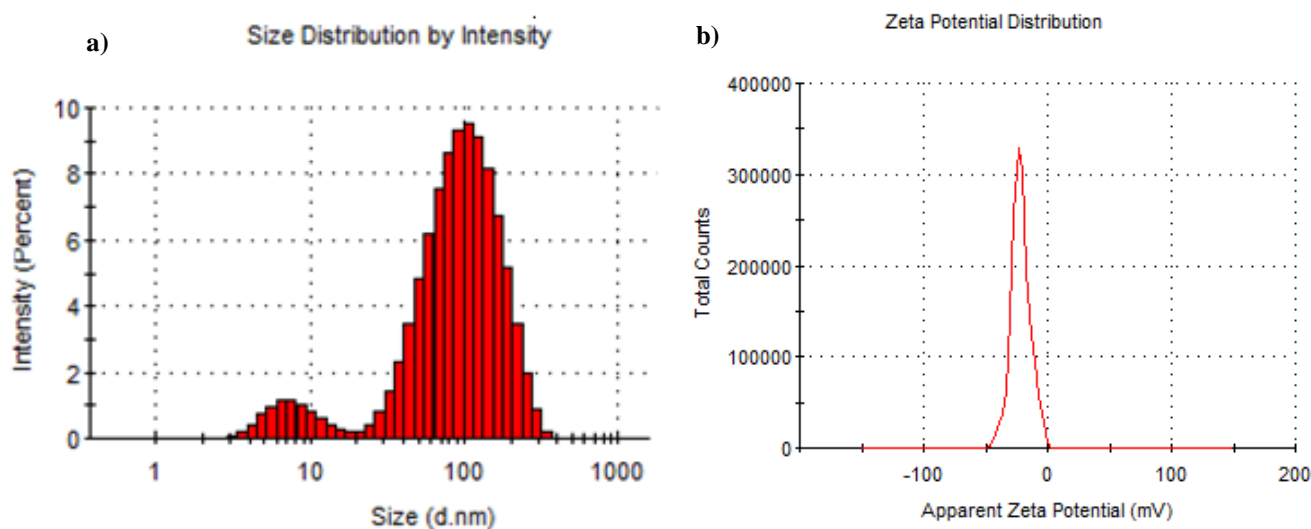

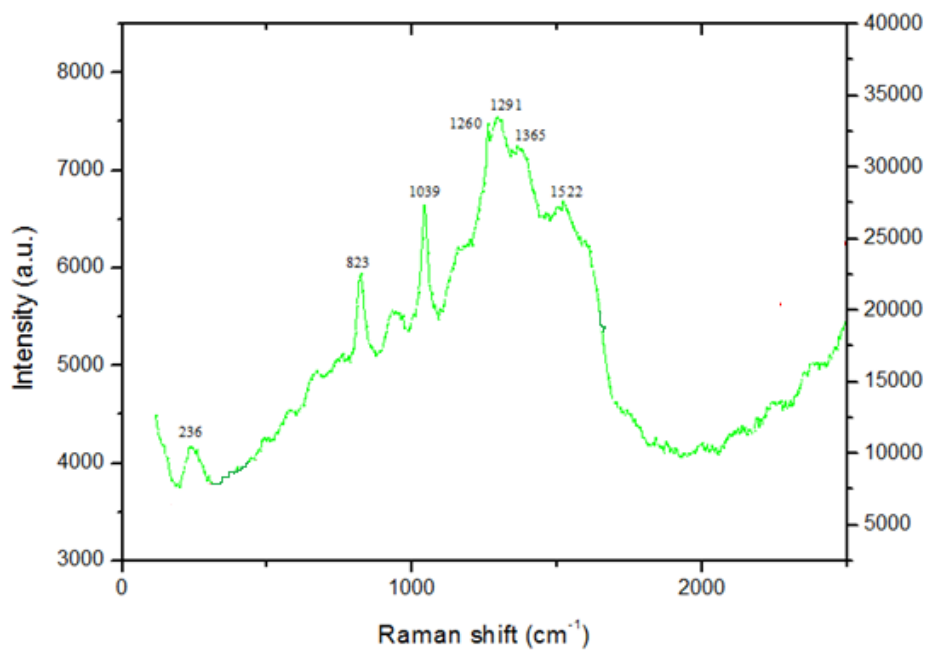**Figure A2.** Distribution of particles size obtained by DLS **(a)** and Zeta potential **(b)** for AgNPs-MI.

Figure A3. Raman spectra of AgNPs-MI.